Hindawi
Geofluids
Volume 2020, Article ID 6687685, 10 pages
https://doi.org/10.1155/2020/6687685

Research Article

Control of Rock Block Fragmentation Based on the Optimization of Shaft Blasting Parameters

Qingxiang Li,[1,2] Zhanyou Luo,[2,3] Man Huang,[1,2] Jiangbo Pan,[4] Guoshu Wang,[4] and Yunxin Cheng[4]

[1]*College of Civil Engineering, Shaoxing University, Shaoxing, 312000 Zhejiang, China*
[2]*Zhejiang Collaborative Innovation Center for Prevention and Control of Mountain Geologic Hazards, Shaoxing, Zhejiang, China*
[3]*Institute of Geotechnical Engineering, Zhejiang University of Science and Technology, Hangzhou, 310023 Zhejiang, China*
[4]*Zhejiang Communications Construction Group Co. LTD, Hangzhou, 310023 Zhejiang, China*

Correspondence should be addressed to Zhanyou Luo; lzy0395@163.com

Received 31 October 2020; Revised 25 November 2020; Accepted 2 December 2020; Published 17 December 2020

Academic Editor: Hang Lin

In the construction of shaft, the blockage of the mucking shaft may cause the mud-water inrush disaster. Oversized rock fragmentation is the main cause for the blockage of the mucking shaft in the raise boring machine (RBM) construction method. The influence degree of blasting parameters on rock fragmentation after blasting is quantified by adopting analytic hierarchy process (AHP). On this basis, the shaft blasting maximum rock fragmentation control model based on double hidden layer BP neural network is proposed. Results show that the maximum rock fragmentation discharged from the mucking shaft after blasting should not exceed 1/3 of the diameter of the slag chute. The influence weight of the minimum resistance line that accounts to 15.6%, when AHP is applied for the quantification of the blasting parameters, can be regarded as the most important blasting parameter. The average absolute errors between the predicted value and the actual value of the largest block size control model of the shaft blasting are only 2.6%. The inversion analysis of the model can rapidly obtain the required blasting parameters, which can be used to guide the construction of the tunnel ventilation shaft.

1. Introduction

Long, large, and deep tunnels have been a trend in tunnel construction, and meeting the requirements of tunnel ventilation and fire smoke exhaust using the single ventilation method has been difficult. The construction of a ventilation shaft has become a reasonable and efficient choice to achieve segmented ventilation [1, 2]. Raise boring machine (RBM) is a popular method that has been adopted in mine shaft construction in recent years [3–5]. In the development of raise boring manufacturing technique and shaft construction technology, the RBM method has been used for large-diameter ventilation shaft construction. The construction of a ventilation shaft with RBM method can be divided into four stages: (1) pilot hole drilling, (2) raise shaft expansion, (3) forward blasting hole expansion, and (4) slipform secondary lining construction [6]. The RBM method has the advantages of the high degree of mechanization, convenient slag extraction, high construction efficiency, and is easy to control quality.

The mucking shaft is the key part in the construction of the RBM method. It is the key to the superiority of the RBM method to other vertical shaft construction methods. However, the mucking shaft is a slender structure and is easy to be blocked during the slag discharge process [7]. Many experts have analyzed the reasons for the blockage of the mucking shaft and have presented methods for prevention and dredging. Hadjigeorgiou et al. considered mucking shaft clogging very common during the construction and operation of shafts in Quebec and Ontario mines in Canada; they also proposed a scheme to use water jets and explosive vehicles to clear the blocker in the mucking shaft [8]. Liu and Li proposed that the small-diameter shaft constructed using the RBM should be expanded in time to eliminate the serious threat to safe production caused by the blockage of the

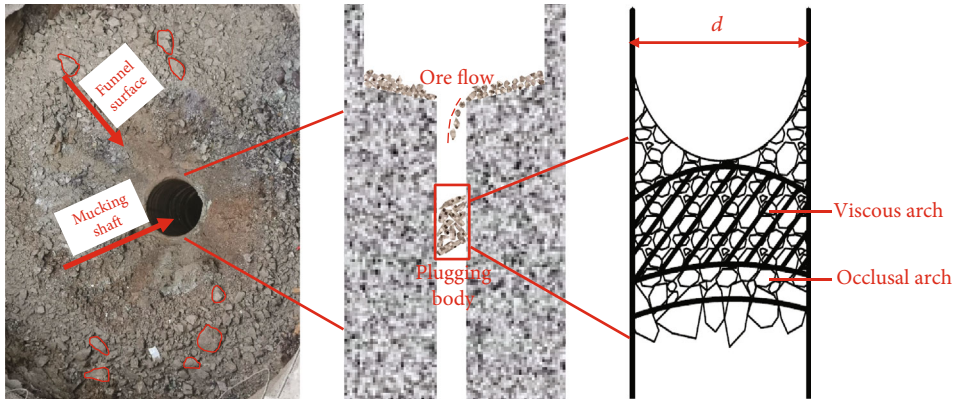

Figure 1

mucking shaft [9]. Peter believed that the ore pass diameter should be between 2.2 m and 3 m and should not be less than 1.8 m; otherwise, blockage in the slagging operation is possible [10]. The aforementioned engineering cases and related studies are based on specific engineering experiences and have focused on passive prevention and dredging after blockage with emphasis on the expansion of the mucking shaft size. In addition, a small number of scholars have proposed an active control method to control the blasting fragmentation by optimizing blasting parameters. Morin and Ficarazzo extended Kuz–Rom model by using Monte Carlo method so that blasting parameters, such as rock and explosive properties, can be used to guide blasting construction and save costs [11]. Wu et al. established a blasting fragmentation prediction model based on the composition analysis method, discriminant classification method, and multiple regression method and predicted the average rock fragmentation (X_{50}); their findings showed that the predicted effect of this model is better than that of the Kuz–Ram model [12]. Ebrahimi et al. used bee colony algorithm and BP neural network to optimize the blasting parameters when the blasting excavation in Anguran mine, Iran, controlled the block size of blasting mining and reduced the back-break phenomenon caused by blasting successfully [13]. Li took the construction of the gas supply shaft at the tail end of the spillway tunnel on the right bank of Xiluodu hydropower station, China, as an example to adjust and control the blasting parameters of the blasting fragmentation to reduce the probability of mucking shaft blockage due to excessive gravel and to ensure the efficiency of the RBM method [14]. The aforementioned blasting fragmentation control methods provide a better solution for the development of engineering projects. However, studies on the maximum rock fragmentation are scarce, and no specific method for controlling the fragmentation of shaft blasting is proposed.

This work investigated the mucking shaft blockage mechanism, quantified the blasting parameters of the shaft based on the analytic hierarchy process (AHP) method, combined it with the construction of the Jinhua mountain tunnel ventilation shaft in China, used the double hidden layer BP neural network algorithm to establish the control model of maximum fragmentation of blasting, and evaluated and analyzed the prediction effect and application methods of the model.

2. Blockage of Mucking Shaft

During blasting, rock failure and other mechanical behaviors under impact load or multistage loading, resulting in different sizes of fragmentation [15, 16]. The mucking shaft is responsible for removing the fissure water and the rock after blasting in the ventilated shaft. Although the structure and function of the mine ore pass vary, the rock movement in the chute is the same. Through blasting, a funnel surface is formed in the shaft face to facilitate slag discharge. The rock is discharged into the mucking shaft manually or mechanically along the funnel surface (Figure 1(a)).

A series of collisions and bounces of ore on the funnel surface will form a stable ore flow (Figure 1(b)). When the ore flow enters the ore pass from the chute, the ore flow has an average velocity as a whole. The initial velocity and lumpiness of the ore flow that enter the ore pass are different; the rocks are easy to squeeze and collide with each other in the shaft [17]. If too many bulk rocks exist, then forming a stable occlusal arch, which will cause cross-sectional blockages, is easy. The formation of the occlusal arch provides a buffer platform for the smaller rocks that fall behind and form a viscous arch under the action of water and lime (Figures 1(d) and 1(e)). The viscous arch is stabilized to form a plugging body because of the impact compaction of the blockage (Figures 1(b) and 1(c)). Therefore, the formation of the plugging body is based on the stable self-standing of the occlusal arch. The formation of the occlusal arch is more complicated. Different rock shapes have various force transmission paths of occlusal arch; thus, analyzing them is difficult.

Szwedzicki [18] believed that the formation of the occlusal arch was mainly related to the degree of rockiness and the diameter of the mucking shaft, and the ratio of the mucking shaft diameter (d) to the rock maximum fragments ($D_{\max}$) was taken as the control, namely,

$$\rho \geq \frac{d}{D_{\max}}. \tag{1}$$

The design section for a mucking shaft drilled by RBM is circular; Hadjigeorgiou and Lessard believed that for a circular vertical chute, the input rocks were sphere to ensure that no stable occlusal arch formed in the well, and the minimum

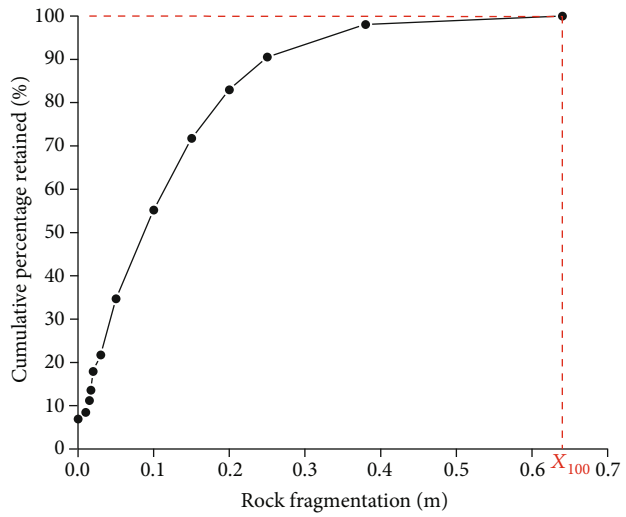

Figure 2

value of ρ is taken as 2.8; if the input rocks are cube, then the minimum value of ρ is 4 [19]. The value of ρ for mucking shaft can be taken as 3, because the shape of the rock mass after blasting is between the two (Figure 1(a)). That is, the rock block size is bigger than 1/3 of the diameter of the mucking shaft. It is defined as a large block, and the secondary crushing is required during the slag discharge.

After blasting, the large rock concentration area on the funnel surface can be taken with a high-pixel camera, and then the rock mass analysis software Split-desktop 4.0 can be used to analyze the rock block fragmentation image; the rock mass distribution result after blasting is shown in Figure 2, and the rock fragmentation distribution data after blasting are obtained. X_{100} is the rock size with a cumulative screen residue of 100%, which represents the maximum rock block fragmentation.

3. Quantification of Blasting Parameters

Blasting parameters are usually optimized to control blasting fragmentation to meet the gradation requirements of mining. However, blasting in the ventilation shaft is different from those in mines. For example, no grading requirement, no cutting hole, and no bench height are provided for the ventilation shaft blasting. Therefore, quantifying the importance of shaft blasting parameters to the formation of blasting fragmentation is necessary.

The AHP is a decision-making method that combines qualitative and quantitative processes [20–22]. Its principle is to decompose complex problems into different hierarchical structures according to the problem-solving steps and compare factors at the same level to form a comparison matrix by calculating the eigenvalues of the comparison matrix of each layer to obtain the weight value of the importance ranking among the factors of each layer and then by calculating the total ranking weight value of all elements. AHP is used to determine the ventilation shaft blasting parameters, which can be divided into five steps.

Step 1. Determine the evaluation factors. The structural model was constructed to analyze the factors that affect blasting fragmentation, and the factors of each layer were coded. Considering the design factors of on-site blasting and the actual situation on site, the blasting design parameters (A_1), rock characteristic parameters (A_2), and performance parameters of explosives (A_3) are selected as the criterion layers of AHP; A_1 include the quantity of blasthole (N), hole spacing (S), hole depth (H), powder factor (P), minimum resistance line (B), and maximum explosive per hole (Q). Rock compressive strength (τ) and rock tensile strength (σ) are the main parameters that can represent rock properties [23, 24]. Meanwhile, detonation velocity (D), explosive action capacity (W), and detonation pressure (C) are selected as the factor layer of A_3. The analysis model shown in Figure 3 is established.

Step 2. Construct a judgment matrix. According to the actual situation of shaft blasting and expert opinions, the reciprocal scale method is used to establish the corresponding comparison matrix S_1, S_2, S_3, and criterion layer matrix S_4 of the factor layer:

$$
\begin{aligned}
S_1 &= \begin{bmatrix} 1 & 0.5 & 1 & 0.25 & 0.33 & 0.33 \\ 2 & 1 & 2 & 2 & 0.33 & 0.5 \\ 1 & 0.5 & 1 & 0.33 & 0.25 & 0.5 \\ 4 & 0.5 & 3 & 1 & 0.5 & 0.5 \\ 3 & 3 & 4 & 2 & 1 & 3 \\ 3 & 2 & 2 & 2 & 0.33 & 1 \end{bmatrix}, \\
S_2 &= \begin{bmatrix} 1 & 4 & 2 \\ 0.25 & 1 & 0.33 \\ 0.5 & 3 & 1 \end{bmatrix}, \\
S_3 &= \begin{bmatrix} 1 & 0.5 \\ 2 & 1 \end{bmatrix}, \\
S_4 &= \begin{bmatrix} 1 & 0.33 & 2 \\ 3 & 1 & 6 \\ 0.5 & 0.17 & 1 \end{bmatrix}.
\end{aligned} \tag{2}
$$

Step 3. Calculate the weight coefficient. Calculate the maximum eigenvalue $\lambda_{\max}$ of the judgment matrix S and the normalized eigenvector to obtain the important weight vector $\boldsymbol{\Omega}$ that affects the blasting parameters:

$$
\begin{aligned}
&\boldsymbol{\Omega}_1 = \{0.069, 0.152, 0.072, 0.157, 0.349, 0.202\}, \lambda_{\max\,1} = 6.3649, \\
&\boldsymbol{\Omega}_2 = \{0.558, 0.122, 0.32,\}, \lambda_{\max\,2} = 3.0183, \\
&\boldsymbol{\Omega}_3 = \{0.333, 0.667\}, \lambda_{\max\,4} = 2, \\
&\boldsymbol{\Omega}_4 = \{0.222, 0.667, 0.111\}, \lambda_{\max\,3} = 3.
\end{aligned} \tag{3}
$$

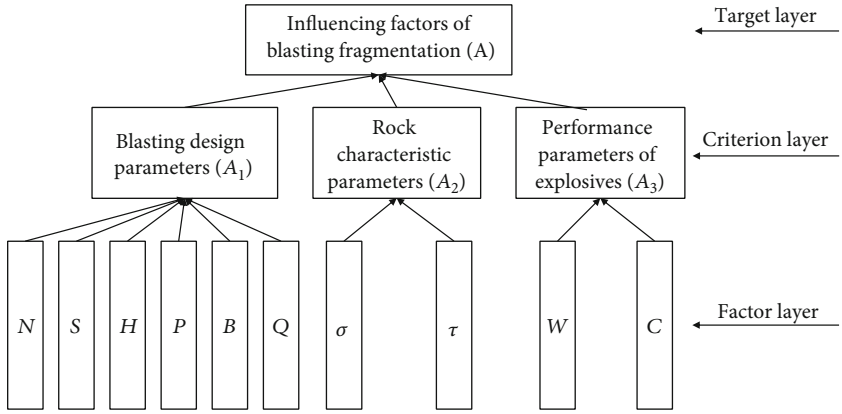

Figure 3

Table 1: Random consistency coefficient.

Matrix dimension	3	4	5	6	7	8	9
RI	0.58	0.9	1.12	1.24	1.32	1.41	1.45

Step 4. Conduct consistency test. To ensure the accuracy of the weight coefficients obtained, the consistency index CI needs to be calculated, and the random consistency coefficient RI is obtained from Table 1, and the random consistency ratio CR can be calculated:

$$\begin{aligned} \mathrm{CI} &= \frac{\lambda_{\max} - n}{n-1}, \\ \mathrm{CR} &= \frac{\mathrm{CI}}{\mathrm{RI}}. \end{aligned} \tag{4}$$

When CR is less than 0.1, it can be considered to pass the consistency test. After calculation, the random consistency ratios of the judgment matrices S_1, S_2, S_3, and S_4 are obtained as follows: 0.0579, 0.0176, 0, and 0, which meet the requirements of the consistency test, respectively.

Step 5. Calculate the comprehensive weight of each level element to the target layer and obtain the ranking of the influence of each blasting parameter on the blasting fragmentation (Table 2).

Table 2 shows that the criterion layer parameters that affect the rock size after shaft blasting are the blasting design parameters (A_1). The most important factor layers are the minimum resistance line (B), maximum explosive per hole (Q), powder factor (P), and the hole depth (H). The cumulative weight value of these factors accounts for 38%, which has a significant impact on the blasting fragmentation. The minimum resistance line comprehensive weight is 15.49%, which should be considered first in the blasting construction.

Table 2: Order of blasting parameter weight.

A	A_1 0.67	A_2 0.22	A_3 0.11	Comprehensive weight	Ranking
B	0.2323	-	-	0.1549	1
Q	0.1347	-	-	0.0898	2
P	0.1047	-	-	0.0698	3
H	0.101	-	-	0.0673	4
τ	-	0.1481	-	0.0329	5
S	0.0479	-	-	0.0319	6
N	0.046	-	-	0.0307	7
σ	-	0.0741	-	0.0165	8
D	-	-	0.062	0.0069	9
C	-	-	0.0355	0.0039	10
W	-	-	0.0136	0.0015	11

4. Maximum Rock Fragmentation Control Model

4.1. Double Hidden Layer BP Neural Network. The BP neural network is a supervised machine learning algorithm that extracts general information or feature information from data through training. Double hidden layer BP neural network is a multilayer artificial neural network that consists of four layers, an input layer, two hidden layers, and an output layer [25] (Figure 4). Each layer is composed of multiple neurons. The double hidden layers increase the number of nodes and the scale of the network and enhance the ability of the neural network to fit nonlinear functions.

4.2. Establishment of Maximum Rock Fragmentation Control Model. The model is based on the double hidden layer BP neural network algorithm. The blasting parameters that affect the fragmentation after blasting, such as the quantity of blast holes, rock tensile strength, and detonation pressure, are used as the input layer to form the input vector set P. Take the corresponding X_{100} as the output set T:

$$\begin{aligned} \mathrm{P} &= \{P_1, P_2, P_3, P_4, P_5 \cdots\}, \\ \mathrm{T} &= \{d_1, d_2, d_3, d_4, d_5 \cdots\}. \end{aligned} \tag{5}$$

The calculation of the blasting maximum fragmentation control model is divided into two processes: the forward

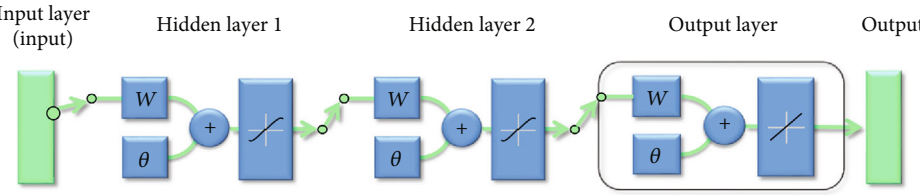

Figure 4

transmission of blasting parameter information and the back propagation of fragmentation error information. The calculation principle is as follows:

If the input and output of the jth neuron in the hidden layer are s_j and b_j, then

$$s_j = \sum_{i=1}^{4} a_i w_{ij} - \theta_j j = 1, 2, 3, \cdots, N, \tag{6}$$

$$b_j = f_1(s_j) j = 1, 2, 3, \cdots, N, \tag{7}$$

$$f_1(x) = \frac{1}{1 + e^{-x}}. \tag{8}$$

In the formula, a_i is the ith input vector in P; w_{ij} and θ_j are the weights and bias value between the input layer and the hidden layer, respectively; formula (8) is the sigmoid function, which is used as the information transfer between neurons.

The input and output of the tth output layer neuron are L_t and C_t, respectively. Then,

$$L_t = \sum_{i=1}^{1} v_{it} b_j - \gamma_t, \tag{9}$$

$$C_t = f_2(L_t), \tag{10}$$

$$f_2(x) = x, \tag{11}$$

where v_{it} and γ_t are the weights and thresholds between the hidden layer and the output layer, respectively. Formula (11) is the activation function between the hidden layer and the output layer.

After the aforementioned calculation, the predicted output value y_t can be obtained, and the error (MSE) between the predicted value and the actual value can be evaluated through the cost function Equation (12) to determine the fit of the model:

$$\text{MSE} = \frac{1}{T} \sum_{t=1}^{T} (y_t - C_t)^2. \tag{12}$$

If the MSE value is less than the default value, then the network training ends or the error will be reduced by back propagation. The calculation is presented as follows:

First, the weights and thresholds of the output layer and hidden layer are adjusted through Equations (13) and (14):

$$v_{jt}(m+1) = v_{jt}(m) + \alpha(y_t - C_t) C_t (1 - C_t) b_j, \tag{13}$$

$$\gamma_t(m+1) = \gamma_t(m) + \alpha(y_t - C_t) C_t (1 - C_t), \tag{14}$$

where m is the number of adjustments of the BP neural network during the training process, α is the adjustment parameter between the hidden layer and the output layer, and the value of α is between 0 and 1. The weight (w_{ij}) and partial quality (θ_j) between the hidden layer and the output layer are readjusted according to Equations (15) and (16):

$$w_{jt}(m+1) = w_{jt}(m) + \beta \left[\sum_{t=1}^{1} (y_t - C_t) C_t (1 - C_t) v_{jt} \right] b_j (1 - b_j) a_j, \tag{15}$$

$$\theta_j(m+1) = \theta_j(m) + \beta \left[\sum_{t=1}^{1} (y_t - C_t) C_t (1 - C_t) v_{jt} \right] b_j (1 - b_j), \tag{16}$$

where β is the learning speed between the input and the hidden layers ($0 < \beta < 1$). The forward information transfer between hidden layer 1 and hidden layer 2 is the same as that between the input layer and hidden layer 1. For hidden layer 2, hidden layer 1 is the input layer, and the same applies to formula (6), (7), and (8); the same is true for back propagation, and the calculation formula satisfies (15) and (16).

The prediction accuracy of the trained neural network model reflects the generalization ability of the model. To represent the accuracy of the model accurately, evaluating the error of the control model after training is necessary. The error is expressed by the average relative error (δ). The calculation formula is as follows:

$$\delta = \sum_{i=1}^{n} \frac{|R_{Pi} - R_{Ci}|}{n R_{Pi}} \times 100\%, \tag{17}$$

where R_{Ci} is the predicted value of the neural network, R_{Pi} is the measured value, and n is the number of input vectors.

5. Application and Discussing

5.1. Case Study. The Jinhua mountain extra-long and deep buried tunnel construction project is located in Jinhua City, Zhejiang Province, China. A vertical ventilation scheme with

Table 3: Geological conditions of the shaft in Jinhua mountain tunnel.

Elevation	Geological conditions	Surrounding rock classification
476.0-467.5	It is a silty clay with gravel, which is loose with block stones distributed locally.	V
467.5-456.0	It is tuff of Huangjian formation or crystal chip fusion, the rock is strongly weathered and locally contains breccia, rock joints and cracks are developed, and the rock quality is hard.	IV
456.0-222.5	It is tuff and crystal debris fusion tuff, which are moderately weathered. The joints and crack are generally developed, thereby showing the block structure mosaic fragmentation. It belongs to hard rock with good integrity. It is locally mixed with tuff silty sandstone, and the rock quality is relatively hard.	III

Table 4: Training parameters of blasting maximum fragmentation model.

Serial number	Elevation	Input parameters							Output parameters
		P	Q (kg)	H (m)	N	S (cm)	τ (MPa)	B (m)	X_{100} (m)
1	472.9	0.80	1.20	2.5	98	0.85	84.3	0.40	0.17
2	471.4	0.87	1.35	2.5	96	0.85	95.3	0.40	0.18
3	467.8	1.14	1.35	3.0	98	0.75	89.3	0.45	0.31
4	465.7	1.05	1.50	3.0	110	0.80	83.0	0.45	0.20
5	464.6	1.00	1.20	2.5	110	0.80	84.2	0.40	0.26
6	462.4	1.20	1.00	2.5	108	0.80	85.5	0.40	0.64
7	451.2	1.31	1.50	3.0	110	0.85	124.4	0.50	0.54
8	449.1	1.50	1.80	3.5	110	0.85	118.0	0.45	0.48
9	446.8	1.50	1.80	3.5	109	0.85	84.2	0.50	0.47
10	444.8	1.65	1.80	3.5	110	0.85	80.7	0.50	0.53
11	442.7	1.70	2.10	3.2	105	0.85	51.3	0.50	0.38

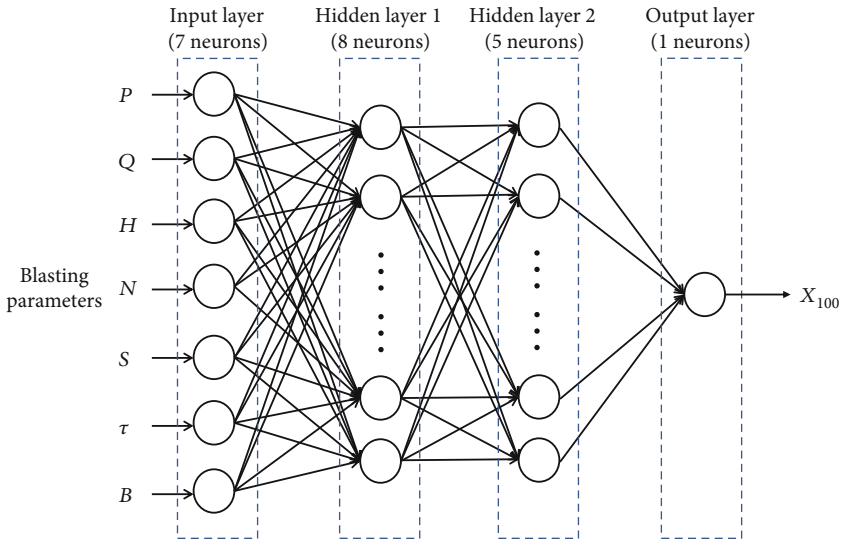

Figure 5

vertical shafts and complementary air ducts is adopted to meet the smoke exhaust and ventilation requirements of the tunnel. The right line of the tunnel uses a vertical shaft for air supply and exhaust, the left line of the tunnel is equipped with a smoke exhaust duct and a normal, natural air duct, and a connecting air duct is set between the left and right lines to achieve complementary ventilation. The central coordinates of the shaft to be constructed is YK2467 +400, the cross-section is circular, the inner contour width is 7.0 m, the diameter of the mucking shaft is 1.5 m, the elevation of the wellhead is 476.0, the elevation of the bottom of the well is 222.5, and the length of the wall is 253.5 m. It belongs to the buried depth, ventilation shaft with large aperture. The shaft spans multiple geological zones (Table 3), and the geological conditions are more complicated. A total of 11 blasting tests were carried out at the construction site during the shaft excavation to prevent the mucking shaft blockage accident during the construction of the shaft. The

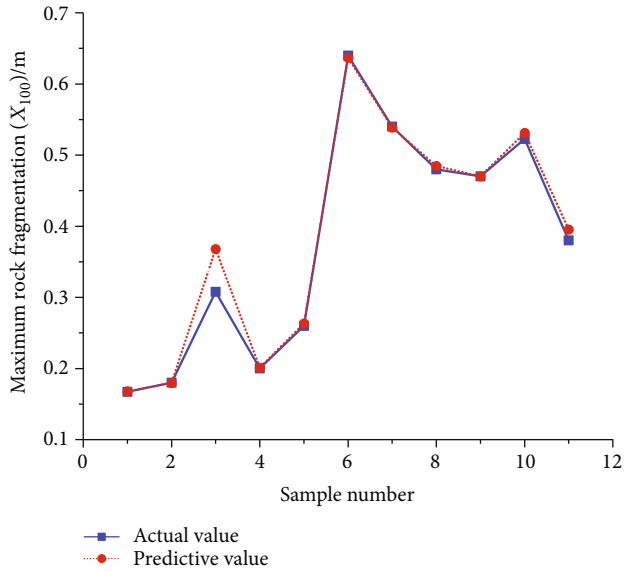

Figure 6

Table 5: Performance indicators of the of two algorithms.

Algorithm	Output	Performance indices		
		Max error (m)	Min error (m)	δ (%)
Single hidden layer	X_{100}	0.06	0.009	7.91
Double hidden layer		0.06	0.0005	2.64

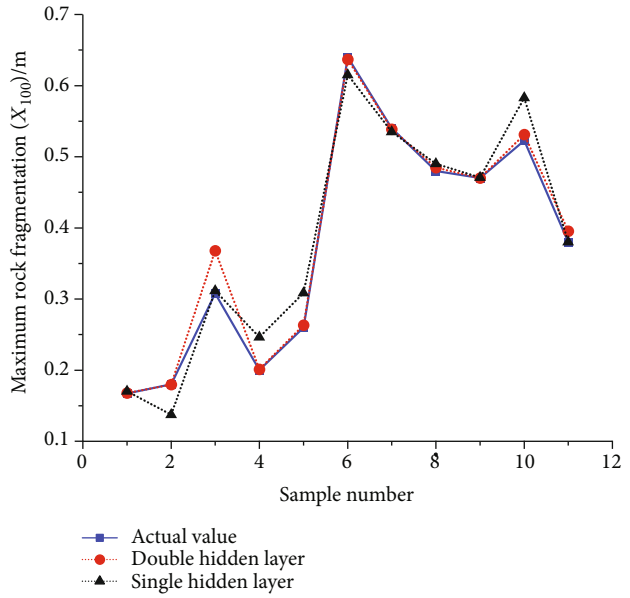

Figure 7

corresponding blasting parameters and rock fragmentation data were collected for the training of the neural network model through the blasting tests. Through the trained model, the maximum blasting fragmentation is predicted, and the maximum fragmentation is controlled to be less than 1/3 of the slag sluice well (0.5 m).

Table 6: Value information of powder factor.

Serial number	Input parameters							Output parameters
	P	Q (kg)	H (m)	N	S (cm)	τ (MPa)	B (m)	X_{100} (m)
1	0.8	1.2	2.5	98	0.85	84.3	0.4	0.17
2	0.89	1.2	2.5	98	0.85	84.3	0.4	0.18
3	0.98	1.2	2.5	98	0.85	84.3	0.4	0.19
4	1.07	1.2	2.5	98	0.85	84.3	0.4	0.21
5	1.16	1.2	2.5	98	0.85	84.3	0.4	0.22
6	1.25	1.2	2.5	98	0.85	84.3	0.4	0.23
7	1.34	1.2	2.5	98	0.85	84.3	0.4	0.24
8	1.43	1.2	2.5	98	0.85	84.3	0.4	0.26
9	1.52	1.2	2.5	98	0.85	84.3	0.4	0.27
10	1.61	1.2	2.5	98	0.85	84.3	0.4	0.29
11	1.70	1.2	2.5	98	0.85	84.3	0.4	0.31

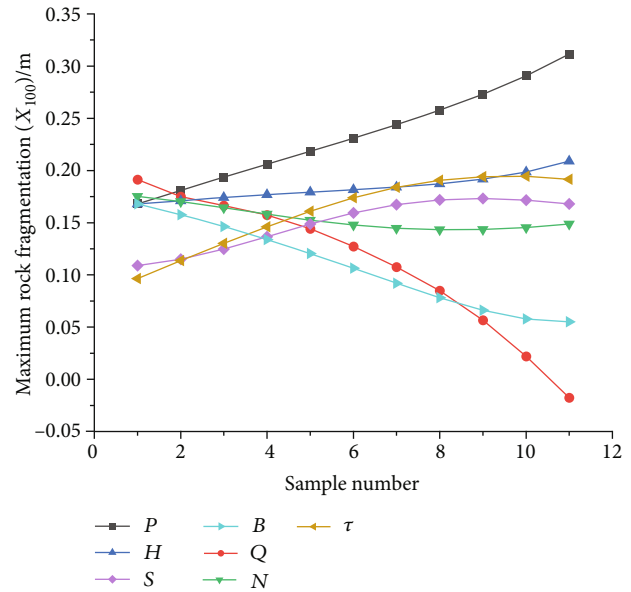

Figure 8

5.2. Data Collection. In the actual blasting operation of the Jinhua mountain shaft, the explosive is fixed to select the emulsion 2# rock explosive. Thus, the explosive parameters are not considered in the input parameter collection. According to the aforementioned research results, the top 7 blasting parameters in Table 2 are selected as the input parameters, and X_{100} is used as the output parameter. The blasting test selects the surrounding rock grades of grade V, grade IV, and grade III because the training effect of the neural network depends on the accuracy of the data to ensure that the fitted blasting maximum fragmentation control model has better generalization ability. This test is carried out under geological conditions. The test data include all the geological conditions of the shaft. The specific test parameters are outlined in Table 4.

Table 7: Parameter inversion data fitting.

Number	Parameter	Fitting	R^2
1	P	$y = 0.15401x + 0.04159$	0.994
2	Q	$y = -0.1792x + 0.38823$	0.943
3	H	$y = x/-4033.13 - 368.1x + 7777.82\sqrt{x}$	0.935
4	N	$y = 0.19139(x - 93.9228)^{-0.10726}$	0.913
5	S	$y = 0.3102(x - 0.73591)^{0.25476}$	0.940
6	τ	$y = \left(-2.65 \times 10^{-3} + 5.8 \times 10^{-5}x\right)^{1/3.3748}$	0.972
7	B	$y = 1.99 \times 10^{-3}x^{-4.90822}$	0.971

5.3. Modeling. According to the aforementioned calculation and analysis processes of the maximum rock fragmentation control model, MATLAB is used to write the corresponding model code to build and train the model. The training data are shown in Table 4. As shown in the maximum rock fragmentation control model in Figure 5, the number of nodes in the first hidden layer of the established model is 8, and the number of nodes in the second hidden layer is 5. The training target is set to 0.001, the learning rate is set to 0.0002, and the training algorithm is the Levenberg–Marquardt algorithm, which is stable and efficient. The training needs to be debugged repeatedly because the BP neural network easily falls into a local minimum, cross-validation is used during training to prevent overfitting. The training set, validation set, and test set are selected randomly, with a ratio of 80%, 10%, and 10%. The accuracy setting value can be added when the program is written to reduce the debugging process; if the accuracy does not meet the set requirements, then the program will return to training automatically until it reaches the set error value; in order to obtain an accurate model, the accuracy confidence interval is set to be 95%. The initial training parameters should be selected carefully; otherwise, the training of the model will easily fail to converge. The 11 groups of blasting parameters in Table 4 are inputted into the trained neural network to simulate the block size prediction. Figure 6 shows that the predicted value is relatively close to the measured value. In Table 5, the average relative error of the model prediction is 2.6%. The maximum error of the rock mass is 0.06 m, and the prediction result meets the engineering needs.

To illustrate the superiority of the double hidden layer neural network model, the prediction effects of the double hidden layer BP neural network model and the traditional single hidden layer neural network are compared. The code of the single hidden layer BP neural network is also written in MATLAB. The training parameters are the same as the two-layer BP neural network, and the same training and test sets are used as the two-layer neural network for network training and testing, respectively. The training results are shown in Table 5 and the two network prediction effects are shown in Figure 7. The fit of dispersion of the prediction data of the double hidden layer BP neural network is significantly higher than that of the single hidden layer BP neural network, indicating that the double hidden layer BP neural network algorithm fits the blasting fragmentation prediction model effectively. The risk of prediction errors is relatively low when this model is applied.

5.4. Application of the Model. Learning the characteristics of existing blasting data, neural network establishes the correlation model between data, the maximum fragmentation of the next blasting can be predicted, and the optimization of the blasting plan is realized by using the model. The rate of the bulk rock block in blasting can be controlled, the occurrence of mucking shaft blockage accidents can be prevented, and the efficiency of shaft construction can be ensured. By using the trained maximum fragmentation control model, the test parameters of the first blasting test in Table 4 (P (0.8), Q (1.2), H (2.5), N (98), S (0.85), τ (84.3), and B (0.4)) are used as the benchmark parameters, and the 7 parameters of the 11 simulated blasting in Table 4 are arranged uniformly from lowest to highest, the 6 remaining parameters remain unchanged, and a group of $7 \times 11 = 77$ blasting parameters can be obtained. The maximum blasting fragmentation that corresponded to the prediction is inputted in the model. Taking powder factor as an example, in Table 4, the minimum value, maximum value and progressive step distance of powder factor are 0.8, 1.7, and 0.09; input the values in into the trained model and obtain the corresponding output parameters (X_{100}). The new prediction groups and results are shown in Table 6. Similarly, get the corresponding values of other parameters.

The prediction result is shown in Figure 8. The compressive strength, hole spacing, and quantity of blastholes gradually decrease with the increase in the parameter values and show a trend of convergence. Powder factor and maximum explosive per hole have great influence on the maximum fragmentation, but the maximum fragmentation of blasting presents an opposite trend with the increase in these two parameters. This instance shows that each parameter has a different degree of influence on the maximum blasting fragmentation. The formation of the maximum blasting fragmentation is the result of the comprehensive action of each parameter. The desired blasting effect cannot be achieved by adding a parameter alone.

In the blasting construction, the blasting parameters need to be adjusted according to the existing conditions. To determine the parameters of the next blasting quickly, 7 sets of blasting parameters fit with the corresponding maximum fragmentation prediction data, and the fitting formulas in

Table 7 are obtained. After certain parameters are determined by using these formulas, other parameters can be deduced quickly according to the required lumpiness.

6. Conclusion

In this paper, the double hidden layer BP neural network algorithm combined with specific engineering examples is used to establish the maximum fragmentation control model of shaft blasting. The conclusions are presented as follows:

(1) The analysis of the ore pass blockage mechanism determined that the excessively large blasting block is the main cause for the blockage of mucking shaft drilled by RBM. Combined with the blockage model of the mucking shaft, the rock fragmentation larger than 1/3 of the diameter of the mucking shaft can be defined as an oversized block that needs to be controlled strictly during on-site construction

(2) As the input parameters of the training maximum size control the model, blasting parameters determine the accuracy of the model. The importance of the blasting parameters of the vertical shaft is quantified by using the AHP. The results show that the four parameters, namely, minimum resistance line, maximum charge per hole, explosive consumption, and hole depth are the main factors that affect the formation of maximum fragmentation in shaft blasting

(3) The construction of the maximum fragmentation control model of shaft blasting based on double hidden layer BP neural network can control the oversized rock proportion effectively. The function relation between each blasting parameter and the maximum fragmentation can be obtained by inverse fitting, and the reasonable blasting parameters can be determined quickly by using the powerful predictive ability of the model, thereby providing an active blocking prevention method to prevent the mucking shaft from blocking. The function relation has practical application significance in engineering

Data Availability

The data used to support the findings of this study are available from the corresponding author upon request.

Conflicts of Interest

The authors declare that there are no conflicts of interest regarding the publication of this paper.

Acknowledgments

The study was funded by the Natural Science Foundation of Zhejiang Province (No. LY18D020003) and Scientific Research Project of Zhejiang Provincial Department of Transportation (No. 2019032). Their support is gratefully acknowledged.

References

[1] Y. Zhuang, H. Ding, G. Zheng, Y. Cui, and Y. Huang, "Study on ventilation system linkage control strategy in a double-hole tunnel fire," *Advances in Materials Science and Engineering*, vol. 2020, Article ID 5163632, 14 pages, 2020.

[2] L. Chai, X. Wang, X. Han, Y. Xia, Y. Wang, and P. Lei, "Optimization method for twin-tunnel complementary ventilation design and its energy saving effect," *Mathematical Problems in Engineering*, vol. 2019, Article ID 6301041, 19 pages, 2019.

[3] A. Shaterpour-Mamaghani, N. Bilgin, C. Balci, E. Avunduk, and C. Polat, "Predicting performance of raise boring machines using empirical models," *Rock Mechanics and Rock Engineering*, vol. 49, no. 8, pp. 3377–3385, 2016.

[4] A. Shaterpour-Mamaghani and N. Bilgin, "Some contributions on the estimation of performance and operational parameters of raise borers–a case study in Kure Copper Mine, Turkey," *Tunnelling and Underground Space Technology*, vol. 54, pp. 37–48, 2016.

[5] A. Shaterpour-Mamaghani, C. Hanifi, D. Engin, and E. Tayfun, "Development of new empirical models for performance estimation of a raise boring machine," *Tunnelling and Underground Space Technology*, vol. 82, pp. 428–441, 2018.

[6] Z. Liu and Y. Meng, "Key technologies of drilling process with raise boring method," *Journal of Rock Mechanics and Geotechnical Engineering*, vol. 7, no. 4, pp. 385–394, 2015.

[7] T. Vo, H. Yang, and A. R. Russell, "Cohesion and suction induced hang-up in ore passes," *International Journal of Rock Mechanics and Mining Sciences*, vol. 87, pp. 113–128, 2016.

[8] F. Hadjigeorgiou, J. F. Lessard, and M. Langevin, "Ore pass practice in Canadian mines," *Journal of South African Institute of Mining and Metallurgy*, vol. 12, no. 11, pp. 813-814, 2005.

[9] S. G. Liu and H. T. Li, "Treatment scheme for blockage of small diameter chute," *Metal Mine*, vol. 438, no. 12, pp. 156-157, 2012.

[10] S. Peter, "Basic considerations and practical experience with the boring of deep shafts by the raise boring process," *Geomechanics and Tunnelling*, vol. 8, no. 1, pp. 50–59, 2015.

[11] M. A. Mario and F. Francesco, "Monte Carlo simulation as a tool to predict blasting fragmentation based on the Kuz–Ram model," *Computers & Geosciences*, vol. 32, no. 3, pp. 352–359, 2006.

[12] R. J. Wu, H. B. Li, C. Yu, and X. Xia, "Model for blasting fragmentation prediction based on statistical classification," *Chinese Journal of Rock Mechanics and Engineering*, vol. 37, no. 1, pp. 141–147, 2018.

[13] E. Ebrahimi, M. Monjezi, M. R. Khalesi, and D. J. Armaghani, "Prediction and optimization of back-break and rock fragmentation using an artificial neural network and a bee colony algorithm," *Bulletin of Engineering Geology and the Environment*, vol. 75, no. 1, pp. 27–36, 2016.

[14] H. Li, "Excavation of vent shaft of discharge tunnel of Xiluodu Hydropower Station," *Yangtze River*, vol. 41, no. 5, pp. 7-8+17, 2010.

[15] Y. Zhao, L. Zhang, W. Wang et al., "Creep behavior of intact and cracked limestone under multi-level loading and unloading cycles," *Rock Mechanics and Rock Engineering*, vol. 50, no. 6, pp. 1409–1424, 2017.

[16] Y. Wang, H. Lin, Y. Zhao, X. Li, P. Guo, and Y. Liu, "Analysis of fracturing characteristics of unconfined rock plate under edge-on impact loading," *European Journal of Environmental and Civil Engineering*, vol. 24, no. 14, pp. 2453–2468, 2020.

[17] Z. Mróz and A. Drescher, "Limit plasticity approach to some cases of flow of bulk solids," *Journal of Engineering for Industry*, vol. 91, no. 2, pp. 357–364, 1969.

[18] T. Szwedzicki, "Formation and removal of hang-ups in ore passes," *Mining Technology*, vol. 116, no. 3, pp. 139–145, 2013.

[19] J. Hadjigeorgiou and J. F. Lessard, "Numerical investigations of ore pass hang-up phenomena," *International Journal of Rock Mechanics and Mining Sciences*, vol. 44, no. 6, pp. 820–834, 2007.

[20] S. Stefanidis and D. Stathis, "Assessment of flood hazard based on natural and anthropogenic factors using analytic hierarchy process (AHP)," *Natural Hazards*, vol. 68, no. 2, pp. 569–585, 2013.

[21] S. Aminbakhsh, M. Gunduz, and R. Sonmez, "Safety risk assessment using analytic hierarchy process (AHP) during planning and budgeting of construction projects," *Journal of Safety Research*, vol. 46, pp. 99–105, 2013.

[22] A. Rezaei and S. Tahsili, "Urban vulnerability assessment using AHP," *Advances in Civil Engineering*, vol. 2018, Article ID 2018601, 20 pages, 2018.

[23] M. Huang, C. J. Hong, S. G. Du, and Z. Y. Luo, "Experimental technology for the shear strength of the series-scale rock joint model," *Rock Mechanics and Rock Engineering*, vol. 53, pp. 5677–5695, 2020.

[24] C. C. Xia, M. Huang, X. Qian, C. J. Hong, Z. Y. Luo, and S. G. Du, "Novel intelligent approach for peak shear strength assessment of rock joints on the basis of the relevance vector machine," *Mathematical Problems in Engineering*, vol. 2019, Article ID 3182736, 10 pages, 2019.

[25] W. Han, L. Nan, M. Su, Y. Chen, R. Li, and X. Zhang, "Research on the prediction method of centrifugal pump performance based on a double hidden layer BP neural network," *Energies*, vol. 12, no. 14, article 2709, 2019.